analytical chemistry

Article

pubs.acs.org/ac

Ratiometric Fluorescence Probe for Monitoring Hydroxyl Radical in Live Cells Based on Gold Nanoclusters

Mei Zhuang, Changqin Ding, Anwei Zhu, and Yang Tian*

Department of Chemistry, Tongji University, Siping Road 1239, Shanghai 200092, People's Republic of China

Supporting Information

ABSTRACT: Determination of hydroxyl radical (•OH) with high sensitivity and accuracy in live cells is a challenge for evaluating the role that •OH plays in the physiological and pathological processes. In this work, a ratiometric fluorescence biosensor for •OH was developed, in which gold nanocluster (AuNC) protected by bovine serum albumin was employed as a reference fluorophore and the organic molecule 2-[6-(4′-hydroxy)phenoxy-3*H*-xanthen-3-on-9-yl]benzoic acid (HPF) acted as both the response signal and specific recognition element for •OH. In the absence of •OH, only one emission peak at 637 nm ascribed to AuNCs was observed, because HPF was almost nonfluorescent. However, fluorescence emission at 515 nm attributed to the HPF product after reaction with •OH—dianionic fluorescein—gradually increased with the continuous addition of •OH, while the emission at 637 nm stays constant, resulting in a ratiometric determination of •OH. The developed fluorescent sensor exhibited high selectivity for •OH over other reactive oxygen species (ROS), reactive nitrogen species (RNS), metal ions, and other biological species, as well as high accuracy and sensitivity with low detection limit to ∼0.68 μM, which fulfills the requirements for detection of •OH in a biological system. In addition, the AuNC-based inorganic−organic probe showed long-term stability against light illumination and pH, good cell permeability, and low cytotoxicity. As a result, the present ratiometric sensor was successfully used for bioimaging and monitoring of •OH changes in live cells upon oxidative stress.

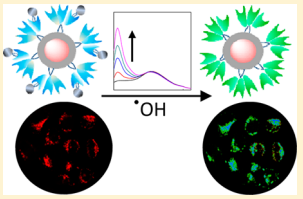

Reactive oxygen species (ROS) have attracted more and more research interest from chemical, biological, and medical fields, because of their important roles in the physiological and pathological events such as aging, cancer, inflammation, regulatory functions, cells signal transduction, and so on.[1] Hydroxyl radical (•OH), belonging to the most reactive chemical species known, shows a short half-life. It is considered to be the most aggressive free radical primarily due to its high reactivity with many different biological species. There is a large amount of evidence that •OH can damage the bases of DNA and mediate redox alteration of cell-membrane Ca^{2+} channels.[2,3] Studies also have shown that •OH is responsible for cellular disorders and could lead to cells apoptosis.[4] In order to further understand the role that •OH plays in biological and pathological events, much more attention has been paid on exploiting highly selective and sensitive methods for real-time and in vivo monitoring of •OH in living systems.

Over the past decades, several elegant techniques have been reported for detection of •OH, such as electron spin resonance (ESR) spectroscopy, ultraviolet−visible (UV−vis) spectroscopy, electrochemical sensing, chromatography, chemiluminescence, and fluorescence spectroscopy.[5−10] Compared with other methods, fluorescence probes provide several advantages such as high specificity and sensitivity, localized information at the target site, even real-time monitoring in living cells, tissues, and animals.[11] Recently, several efficient fluorescent sensors for detection of •OH were reported.[12] However, development of ratiometric fluorescence probes for intracellular •OH measurement is still limited by the design of dual-emission organic fluorophores which should be specific and sensitive to •OH. Actually, the ratiometric sensor has attracted significant attention as an alternative to first-generation intensity probes due to its sensitivity and the built-in correction for avoiding environmental effects. In the present work, we first integrated gold nanoclusters (AuNCs) with a specific molecule, 2-[6-(4′-hydroxy)phenoxy-3*H*-xanthen-3-on-9-yl]benzoic acid (HPF), for •OH,[13] thus developed a selective and sensitive ratiometric fluorescent probe for •OH. As demonstrated in Scheme 1, in this ratiometric probe, the unfluorescent organic molecule HPF was employed as both the specific recognition element and response signal for determination of •OH due to the increasing fluorescence of the HPF product at 515 nm after specifically being reacted with •OH, while AuNCs emitting at 637 nm served as reference signal for providing built-in correction to avoid environmental effects because of the good stability even in the presence of •OH.

Gold nanoclusters are new type of luminescent nanomaterials and have recently drawn great interest in the fields of catalysis, sensors, and biomedical imaging.[14] Gold nanoclusters have sizes comparable to the Fermi wavelength of electrons and give rise to molecule-like properties including discrete electronic states and size-dependent fluorescence.[15] So far, protein, peptides, and thiol compounds were used to prepare AuNCs in general.[16−18] Gold nanoclusters protected by bovine serum albumin (BSA) also show good photoluminescence properties,[16a] which can be excited by visible light (400−520

Received: November 24, 2013
Accepted: January 3, 2014
Published: January 3, 2014

   dx.doi.org/10.1021/ac403810g | *Anal. Chem.* 2014, 86, 1829−1836

Scheme 1. (a) Working Principle of the Developed AuNC@HPF Fluorescent Probe for •OH Detection; (b) Reaction Scheme of HPF with •OH

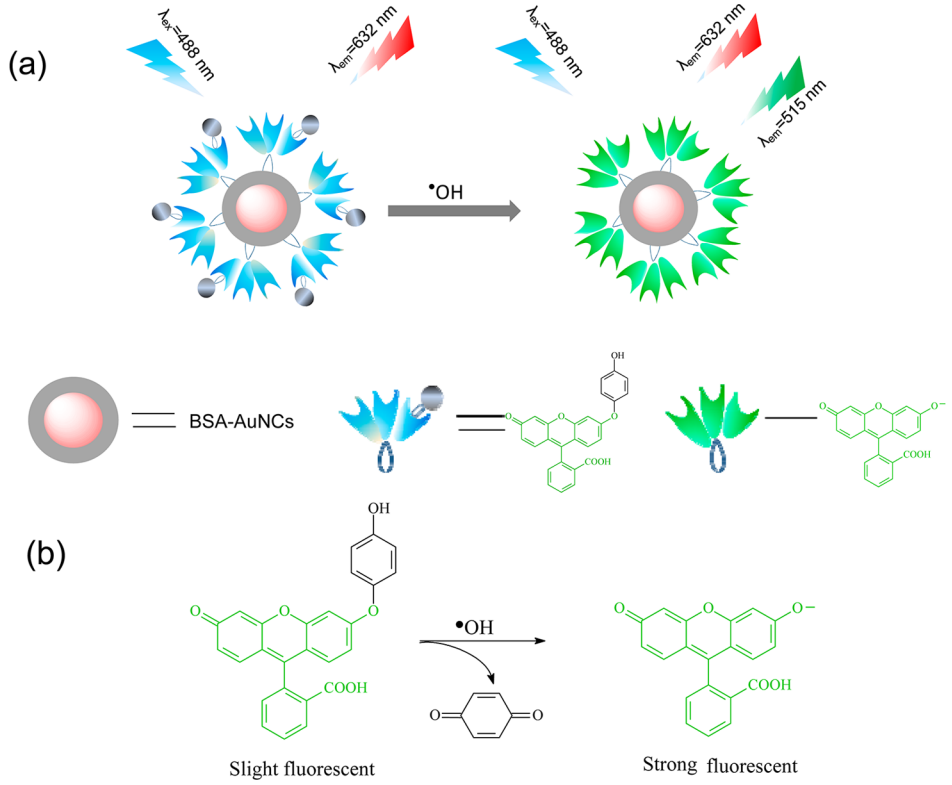

nm) and emit with a large Stokes shift (637 nm). Meanwhile, BSA-protected AuNCs exhibit good biocompatibility, low cytotoxicity, and small size down to ~2−3 nm, in comparison with quantum dots (QDs).[19] Thus, AuNCs are more attractive and potentially useful for bioimaging and biosensing in live cells. In this work, AuNCs protected by BSA with amine groups were employed as reference signal and conjugated with carboxyl groups of HPF to form a ratiometric fluorescence probe AuNC@HPF. Here, HPF acted not only as the specific recognition element for •OH, but also as a response signal, because nonfluorescent HPF can specifically react with •OH to generate the product—dianionic fluorescein—which emitted at 515 nm. In addition, the green fluorescence of dianionic fluorescein gradually increased with the increasing concentration of •OH, while the red fluorescence ascribed to AuNCs at 637 nm remained constant, resulting in the ratiometric determination of •OH using the inorganic−organic AuNC@HPF probe. Because of the specific recognition of HPF with •OH, the developed probe showed high selectivity for •OH detection over typical ROS, RNS, metal ions, and other biological species. Meanwhile, the ratiometric fluorescence biosensor was sensitive to •OH in a the range from 1 to 150 μM with a low detection limit of ~0.68 μM. Compared with previous ratiometric probes for •OH,[20−23,25] the present fluorescent probe also showed good water solubility and cell permeability, low-cytotoxicity and high biocompatibility, and long-term stability against light illumination and pH, thus was successfully applied for bioimaging and monitoring of •OH changes in Hela cells exposed to oxidative stress.

EXPERIMENTAL SECTION

Reagents and Chemicals. Gold(III) chloride trihydrate ($HAuCl_4 \cdot 3H_2O$, 99%), HPF, dimethyl sulfoxide (DMSO), 1-ethyl-3-(3-dimethylaminopropyl)carbodiimide (EDC), *N*-hydroxysuccinimide (NHS), methyl thiazolyl tetrazolium (MTT), and lipopolysaccharides (LPS) from *Escherichia coli* were purchased from Sigma-Aldrich. Hydrogen peroxide (30%), sodium nitrite, sodium hypochlorite, potassium superoxide, and 2,2′-azobis(2-methylpropionamidine)-dihydrochloride (AAPH) were obtained from Aladdin Chemistry Co. Ltd. Albumin from bovine serum (BSA), amino acids, glucose, potassium dihydrogen phosphate, potassium phosphate dibasic trihydrate, and sodium hydroxide, were obtained from Sinopharm Chemical Reagent Co. Ltd. Solutions of metal ions were all prepared from their chloride salts. Dialysis tube (MWCO: 3500) was obtained from Ebioeasy Corporation. Hoechst 33342 and cell culture media and supplements were supplied by Invitrogen Corporation. Apoptosis assay was implemented by an Annexin V-FITC apoptosis detection kit. Double-distilled deionized water was obtained from a Millipore water purification system.

Instruments and Methods. UV−vis (Agilent 8453) was used to measure the optical absorption spectra. Transmission electron microscopy (HR-TEM, JEOL 2100, Japan) was employed to observe the morphology of AuNCs operating at 200 kV. X-ray photoelectron spectroscopy (XPS, PHI5000 ESCA, Perkin-Elmer, U.S.A.) equipped with an Al Kα source (1486.6 eV photons) was used to characterize the AuNCs. Fourier transform infrared spectroscopy (FT-IR, Nicolet 6700, Thermo Electron, America) was used to characterize the conjugation of HPF and AuNCs. Fluorescence spectrum (F-2700FL, Hitachi, Japan) was used to measure the fluorescence

dx.doi.org/10.1021/ac403810g | *Anal. Chem.* 2014, 86, 1829−1836

spectrum and determine the relationship between fluorescence and the concentration of hydroxyl radical (•OH) generated by Fenton reagent. Confocal laser scanning images were obtained at a confocal laser scanning biological microscope (Fluoview 1000, Olympus, Japan).

Preparation of AuNCs and AuNC@HPF. BSA-stabilized AuNCs were prepared according to a green biomineralization synthetic method.[16a] Briefly, 5 mL of 10 mM $HAuCl_4$ solution was added to 5 mL of 50 mg mL^{-1} BSA solution under vigorous stirring at 37 °C. Two minutes later, 0.5 mL of NaOH solution (1 M) was added and the reaction was continued under vigorous stirring at 37 °C for 12 h. Then, AuNCs solution was obtained and dialyzed in ultrahigh-purity water for 24 h (changing the water every 8 h). At last, the as-prepared AuNCs were stored at 4 °C for further used (25 mg mL^{-1}). In order to get a more concentrated solution, a freeze-dryer was used, and the solid AuNCs could be redispersed in ultrapure water or PBS buffer (pH = 7.4).

Then, to conjugate HPF on AuNCs surface, 10 μL of HPF (5 mM) was introduced into 3.6 mL of PBS (0.05 M, pH = 7.4) with 10% DMF[24] and activated by 0.0400 g of EDC and 0.0400 g of NHS for 2 h. Then, 400 μL of AuNCs solution was added. The reaction was finished after 10 h. Finally, the nanohybrid was separated from the byproduct of the reaction and unreacted HPF by dialysis in PBS (0.05 M, pH = 7.4) for 8 h using dialysis tube (MWCO: 3500). The dialysis membrane has been widely used to remove small-size molecules such as Na^+, OH^-, Cl^-, and other reaction coproducts generated in the synthesis process of AuNCs. More importantly, in the present work, this dialysis membrane MWCO was employed to remove remaining free HPF. The product was denoted as AuNC@HPF, and the standard solution (2.5 mg mL^{-1}) was stored at 4 °C. All the process should be kept in the refrigerator.

Fluorescence Spectroscopy. In the fluorescence assay, a cuvette with the length of 1 cm was used. The sample was excited at 488 nm, and the emission was collected from 500 to 750 nm. The experiments for •OH detection were all carried out three times. To detect •OH by AuNC@HPF probe, 1 mL of standard solution (pH = 7.4) was first added into the cuvette, then •OH was generated through Fenton reaction by different amounts of Fe^{2+} and H_2O_2 (Fe^{2+}/H_2O_2 = 1:6). After incubation with the probe for 15 min,[12a] the fluorescence spectrum was obtained at an F-2700FL instrument.

For the selectivity experiment, hydroxyl radical (•OH) was generated by the Fenton reaction (Fe^{2+}/H_2O_2 = 150 μM, 900 μM). Superoxide anion ($O_2^{\bullet-}$) derived from dissolved KO_2 (150 μM) in the DMSO solution. Hypochlorite anion (ClO^-) was provided by NaClO (150 μM). Alkyl peroxyl radical ($ROO^\bullet$) was chemically generated by thermolysis of AAPH (150 μM) in air-saturated aqueous solution at 310 K. Peroxynitrite ($ONOO^-$) was chemically generated by the reaction between H_2O_2 (150 μM) and $NaNO_2$ (150 μM). Nitric oxide (NO) and nitroxyl (HNO) derived from the solution of *S*-nitroso-*N*-acetyl-DL-penicillamine and Angeli's salt, respectively. $^1O_2$ was generated by the reaction of H_2O_2 (150 μM) with NaClO (150 μM). All experiments were obtained after incubation with the appropriate ROS/RNS for 30 min at room temperature.

MTT Assay. The cellular cytotoxicity of AuNC@HPF was tested on Hela cells. First, the culture medium was removed and the Hela cells were incubated in culture medium including the AuNC@HPF probe in the concentrations of 0.025, 0.25, 2.5, 25, and 100 μg mL^{-1} for 24 and 48 h, respectively. Then cells were washed with the culture medium, and 100 μL of the new culture medium containing MTT (10 μL, 5 mg mL^{-1}) was added to each well followed by incubation for 4 h to allow the formation of formazan dye. Finally, the supernatant was removed before 150 μL of DMSO was added to each well, and the plate was shaken for 10 min. By measuring the absorbance at 490 nm using an enzyme-labeling instrument (EX-800 type) in quintuplicate, the cell viability values were determined (five times) according to the following formula: cell viability (%) = the absorbance of experimental group/the absorbance of blank control group × 100%.

Apoptosis Assay. Hela cells were incubated with AuNC@HPF at the concentrations of 0.025, 0.25, 2.5, 25, and 100 μg mL^{-1} for 24 h. Cells floating in the cell medium were collected by centrifuge while adherent cells were collected by treating with trypsin−EDTA. After washing with PBS, cells were then stained with FITC−annexin V (Molecular Probe) and propidium iodide (PI, Aldrich) following the standard protocol. The flow cytometry (FACS) measurements were collected from a Becton-Dickinson flow cytometer.

Cell Culture. Hela cells were cultured in Dulbecco's modified Eagle's medium (DMEM) including high glucose supplemented with 10% (v/v) fetal bovine serum, penicillin (100 units mL^{-1}), and streptomycin (100 μg mL^{-1}). Hela cells (~3 × 10^5 cell mL^{-1}) were seeded onto a 96-well microliter plate to a total volume of 100 μL/well in an atmosphere of 5% CO_2 and 95% air at 37 °C humidified incubator for 24 h.

Fluorescence Imaging and Biosensing. First, one day before imaging studies, the cultured cells were passaged and plated on a Petri dish. The cells were incubated for ~1 h at 37 °C in the culture media (2 mL) containing 2 μL of AuNC@HPF standard solution. The cells were washed with Hank's balanced salt solution (HBSS) (pH = 7.4), and the process was repeated three times. Then, the cells were cultured in 2 mL of HBSS (pH = 7.4) during the imaging experiments. The cell fluorescence imaging was obtained with an Olympus FV1000 confocal laser scanning microscope equipped with an oil immersion 60× objective. Using an excitation wavelength at 488 nm, the images of the HPF channel were obtained in the 500−560 nm detection range, and the images of the AuNCs channel were collected in the 580−690 nm range. In order to detect the •OH generated in cells, LPS (10 μg mL^{-1}) was introduced to induce oxidative stress,[25] and then fluorescence microscopic images were acquired after different minutes.

RESULTS AND DISCUSSION

Characterization of AuNCs and AuNC@HPF. BSA-stabilized AuNCs were synthesized according to a green biomineralization method.[16a] From the TEM image shown in Figure 1A, the as-prepared AuNCs showed to be monodispersed with average size of ~3 nm. As demonstrated in Figure 1B, XPS result for Au $4f_{7/2}$ can be deconvoluted into two components centered at Au^0 (83.7 eV) and Au^{1+} (85.0 eV), respectively, which are in a good agreement with that previously reported AuNCs.[16a] The FT-IR spectrum of the AuNCs is shown in Figure 1C (curve a). Three peaks located at 3452 cm^{-1} (ν_{O-H}), 1657 cm^{-1} ($\nu_{C=O}$), and 1546 cm^{-1} (ν_{N-H}) were observed. The presence of these hydrophilic groups including $-NH_2$, −COOH, and/or −OH imparts AuNCs surrounded by BSA water solubility. On the other hand, the FT-IR spectrum for HPF (Figure 1C, curve b) shows three characteristic peaks located at 1102, 984, and 863 cm^{-1}, which are ascribed to the vibration of C−O−C, C═C, and C−H of

dx.doi.org/10.1021/ac403810g | Anal. Chem. 2014, 86, 1829−1836

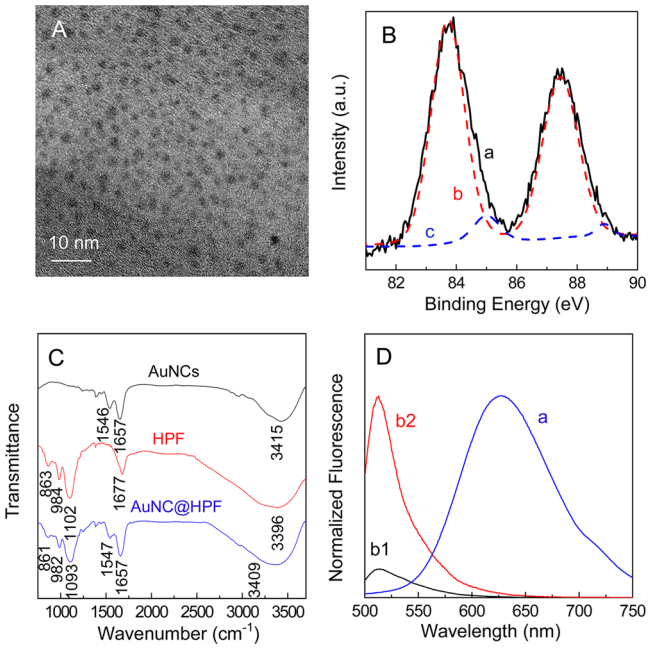

Figure 1. (A) TEM image of AuNCs. (B) X-ray photoelectron spectroscopy of AuNCs. (C) FT-IR spectra of (a) the as-prepared AuNCs, (b) HPF, and (c) AuNC@HPF. (D) Normalized fluorescence spectra of (a) AuNCs, (b1) HPF, and (b2) the product of HPF after being reacted with •OH (dianionic fluorescein) (488 nm excitation).

alkene, respectively. Six peaks were clearly observed at 3409 cm^{-1} (ν_{O-H}), 1657 ($\nu_{C=O}$), 1547 (ν_{N-H}), 1093 cm^{-1} (ν_{C-O-C}), 982 cm^{-1} ($\nu_{C=C}$), and 861 cm^{-1} (ν_{C-H}) in the FT-IR spectrum of AuNC@HPF (Figure 1C, curve c), which suggests the successful attachment of HPF onto the surface of AuNCs.

The fluorescence emission peak for AuNCs was observed at 637 nm, as shown in Figure 1D curve a, under excitation at 488 nm. Using rhodamine B as a standard, the fluorescence quantum yield (QY) of AuNCs was estimated to be ~5% excited at 488 nm (Figure S1, Supporting Information).[26] Actually, HPF exhibited negligible fluorescence emission upon excitation of 488 nm (Figure 1D, curve b1). However, after being reacted with •OH, the product of HPF (dianionic fluorescein) emitted with a fluorescence peak at 515 nm (Figure 1D, curve b2). As previously reported, the phenoxyl radical form of HPF formed by interaction with •OH can undergo self-reaction, or reaction with •OH leading to the formation of radical coupling products from which the release of the fluorescent product may take place.[27] As expected, the inorganic−organic nanohybrid AuNC@HPF showed only one obvious fluorescence peak at 637 nm upon excitation at 488 nm in the absence of •OH (inset in Figure 2A, curve a1). With the addition of •OH, the fluorescence peak at 515 nm attributed to the product of HPF after being reacted with •OH appeared, while the fluorescence peak at 637 nm ascribed to AuNCs stays constant, resulting in the ratiometric detection of •OH (inset in Figure 2A, curve a2).

Analytical Performance of AuNC@HPF Probe for •OH Detection. In this ratiometric probe, the organic molecule HPF was used as both the specific recognition element and response signal for determination of •OH due to the increasing fluorescence intensity of the HPF product with the specific reaction with •OH, while AuNCs served as the reference signal because of the good stability even in the presence of •OH. The mass concentration ratio between AuNCs and HPF was optimized as shown in Figure S2 (Supporting Information). The response of the optimized ratiometric AuNC@HPF fluorescent probe toward •OH was then carried out to prove the working principle, as demonstrated in Figure 2. Hydroxyl radical was generated by adding different concentrations of Fe^{2+} and H_2O_2 (1:6) with a reaction time of 15 min (Figure S3, Supporting Information). As shown in Figure 2A, in the absence of •OH, only one peak was clearly observed at 637 nm, while HPF showed negligible fluorescence. However, after HPF reacted with •OH, the fluorescence peak at 515 nm appeared, which was not observed when only Fe^{2+} or H_2O_2 was added in the solution (Figure S4, Supporting Information). These results indicate that the fluorescence peak located at 515 nm was ascribed to the HPF product—dianionic fluorescein. Furthermore, the fluorescence intensity at 515 nm gradually increased with the increasing concentrations of •OH, while the fluorescence peak at 637 nm almost remained constant. As demonstrated in Figure 2B, the dual-emission fluorescence intensity ratio ($I_{500-560}/I_{580-690}$) increased linearly with the concentration of •OH in the range of 1×10^{-6} to 1.5×10^{-4} M [$Y = 0.2416 + 0.02138X$ ($R^2 = 0.998$)], with a detection limit of ~0.68 μM (based on a signal-to-noise ratio of S/N = 3). This AuNC@HPF ratiometric probe provided a built-in correction for avoiding the environmental effects. Compared with those reported ratiometric •OH probe,[20−23] the present inorganic−

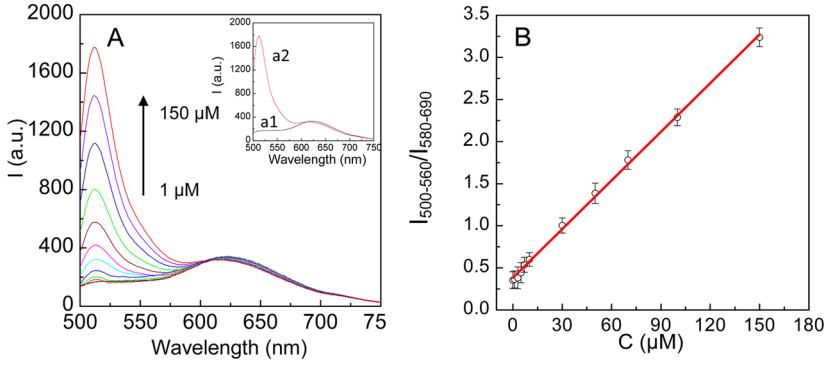

Figure 2. (A) Fluorescence spectra of the ratiometric probe upon the exposure to different concentrations of •OH at various Fe^{2+} concentrations (0, 1, 3, 5, 7, 10, 30, 50, 70, 100, 150 μM) (488 nm excitation). Inset: (a1) blank fluorescent spectrum of AuNC@HPF probe and (a2) fluorescent spectrum of AuNC@HPF probe after being reacted with •OH. (B) The plot of $I_{500-560}/I_{580-690}$ as the function of •OH generated by Fenton reaction.

dx.doi.org/10.1021/ac403810g | Anal. Chem. 2014, 86, 1829−1836

organic probe showed higher sensitivity and lower detection limit.

The complexity of the intracellular system presents a great challenge for biosensors not only in sensitivity but more importantly in selectivity. The selectivity experiments were carried out by monitoring the intensity ratio ($I_{500-560}/I_{580-690}$) of the probe in the presence of typical ROS and RNS, metal ions, and other biological species, which may coexist in the living system. Remarkably, as demonstrated in Figure 3A,

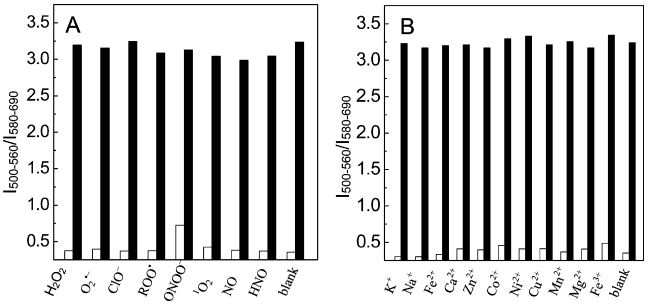

Figure 3. (A) Fluorescence responses of AuNC@HPF probe in PBS (pH = 7.4) upon 488 nm excitation toward different ROS and RNS including H_2O_2 (900 μM), $O_2^{\bullet-}$ (150 μM), ClO$^-$ (150 μM), ROO$^\bullet$ (150 μM), ONOO$^-$ (150 μM), $^1O_2$ (150 μM), NO (150 μM), and HNO (150 μM). The white bars represent the addition of ROS and RNS to the fluorescent probe. The black bars represent the subsequent addition of 150 μM $^\bullet$OH to the fluorescent probe. (B) Fluorescence responses of AuNC@HPF in PBS (pH = 7.4) upon 488 nm excitation toward different metal ions: K^+ (1 mM), Na^+ (1 mM), Fe^{2+} (150 μM), Ca^{2+}(10 μM), Zn^{2+} (10 μM), Co^{2+} (10 μM), Ni^{2+} (10 μM), Cu^{2+} (10 μM), Mn^{2+} (10 μM), Mg^{2+} (10 μM), Fe^{3+} (10 μM). The white bars represent the addition of different ions to the probe solution. The black bars display the subsequent addition of 150 μM $^\bullet$OH to the fluorescent probe.

unperturbed fluorescence responses (<5%) were observed for typical ROS and RNS such as superoxide anion radical ($O_2^{\bullet-}$), hypochlorite (ClO$^-$), alkylperoxyl radical (ROO$^\bullet$), peroxynitrite (ONOO$^-$), nitric oxide (NO), nitroxyl (HNO), single oxygen ($^1O_2$), and H_2O_2, compared with that obtained for $^\bullet$OH. Furthermore, these potential ROS and RNS interferences showed negligible effects on the signal for $^\bullet$OH sensing. In addition, no obvious responses were obtained for the metal ions (Figure 3B) and other biological species including amino acids and glucose (Figure S5 in the Supporting Information), and little effect on the intensity ratio of the probes was observed after their exposure to 10 μM concentrations of metal ions and so on. These experiments demonstrated that the present inorganic–organic fluorescence probe had high selectivity for $^\bullet$OH determination against ROS and RNS, metal ions, and other biological species. Furthermore, the present ratiometric probe was independent of solution pH in the biologically relevant pH from 6.5 to 8.5 (Figure S6 in the Supporting Information), which fulfills the requirement for monitoring of $^\bullet$OH in the biological system.

Stability and Cytotoxicity. The photostability of the AuNC@HPF probe was then investigated, and the result is summarized in Figure 4A. The fluorescent probe was exposed to a fluorescence spectrophotometer (λ_{ex} = 488 nm) equipped with a 90 W xenon lamp for 3600 s, and the dual emissions at 515 nm (I_{515}) and 637 nm (I_{637}) were measured three times to evaluate the stability. As shown in Figure 4A, no obvious changes (<5%) were observed for the ratio I_{515}/I_{637} after 1 h of

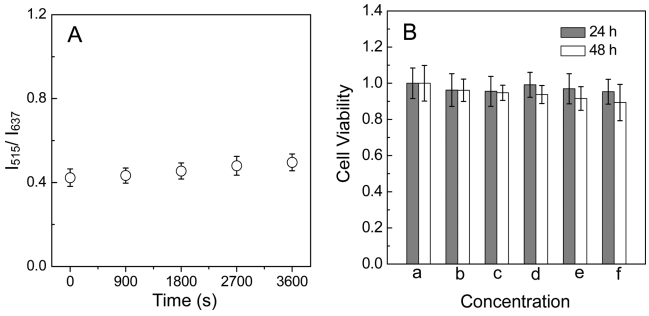

Figure 4. (A) Photostability of the AuNC@HPF probe measured by fluorescence spectrophotometer for three times. (B) Cells viability values (%) estimated by MTT proliferation tests. Hela cells were incubated with the concentrations of AuNC@HPF of (a) 0, (b) 0.025, (c) 0.25, (d) 2.5, (e) 25, and (f) 100 μg mL^{-1} for 24 (gray) and 48 h (white) at 37 °C, respectively.

being exposed to the radiation, suggesting the good photostability of this inorganic–organic fluorescent probe.

For further biological application, the long-term cellular toxicity of AuNC@HPF toward Hela cell lines was determined by means of a standard MTT assay. In the presence of the present probe with concentration from 0.025 to 100 μg mL^{-1}, the cellular viabilities were estimated to be greater than ~95% and ~90% after incubation for 24 and 48 h, respectively, as demonstrated in Figure 4B. The results indicate that the AuNC-based probe is generally low toxic for cellular imaging, possibly due to good biocompatibility of the surrounded biomolecule BAS. The conclusion was also supported by the results of flow cytometry experiments. Apoptosis assay of Hela cells after AuNC@HPF probe treatment was carried out to evaluate the biocompatibility by FACS measurements. Taking Hela cells as an example, they were first incubated with AuNC@HPF at concentrations of 0.025, 0.25, 2.5, 25, and 100 μg mL^{-1} for 24 h. Then, the cells were stained by FITC–annexin V and PI to label the apoptosis cells and necrotic cells, respectively, for FACS measurement. As shown in Figure 5, there are no obvious differences between control cells and the cells treated with the present probe, demonstrating high biocompatibility of the AuNC@HPF probe.

Bioimaging and Biosensing of $^\bullet$OH in Live Cells. As demonstrated above, the AuNC@HPF probe shows high selectivity and sensitivity, as well as long-term stability and low cytotoxicity. The enhanced analytical performance, together with the remarkable properties of this AuNC-based ratiometric fluorescent probe substantially provides a reliable platform for bioimaging and biosening of $^\bullet$OH in live cells. First, AuNC@HPF probe was incubated with Hela cells in cell culture media for 1 h and then washed with HBSS for three times to remove the remaining probe in cell culture media. After the uptake, the probe was monitored by confocal microscopy upon 488 nm excitation. From the overlay images (Figure 6C) of the confocal fluorescence image and bright-field image (Figure 6B), it is clear that the probe had good cell permeability and entered the cell membrane easily. Meanwhile, from the nuclear staining experiment, which was carried out using Hoechst 33342[28] as the nucleus stain, we found the AuNC@HPF probes were located in cytoplasm and near the cell nucleus (Figure S7 in the Supporting Information). The fluorescence scan in Hela cells treated with AuNC@HPF (Figure 6D) probes also confirmed that the present probes maintained the dual emission located at ~515 and ~637 nm in a cellular environment.

dx.doi.org/10.1021/ac403810g | Anal. Chem. 2014, 86, 1829–1836

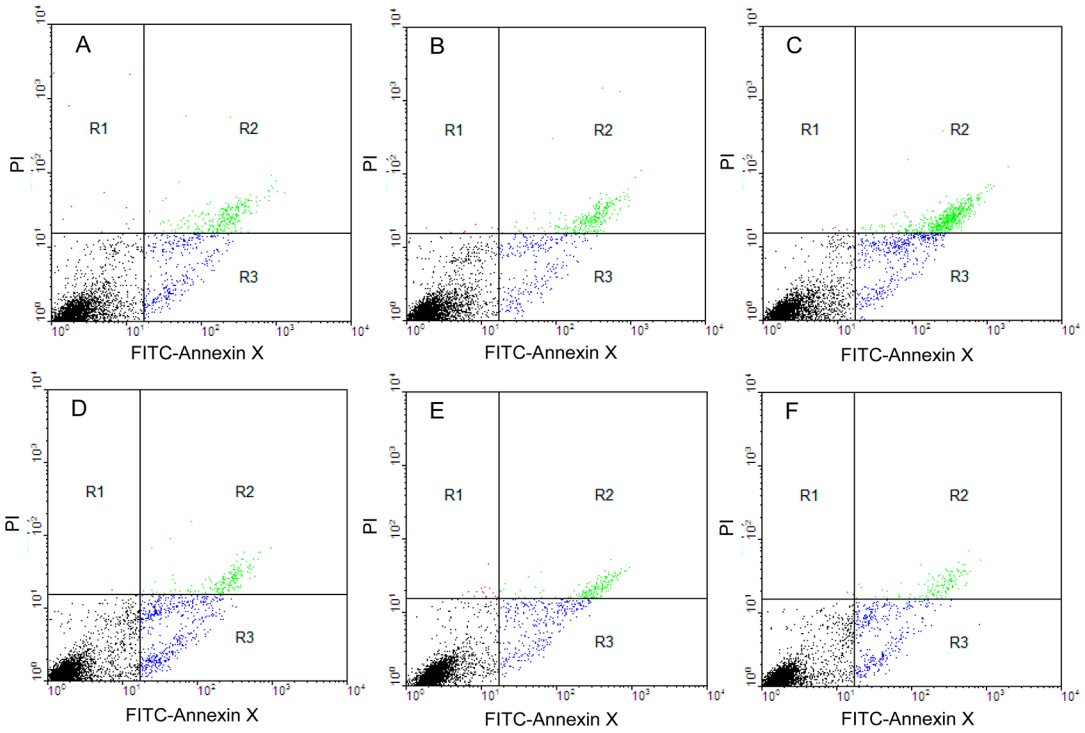

Figure 5. Apoptosis assay of Hela cells after AuNC@HPF treatment. Hela cells were incubated with AuNC@HPF at concentrations of (A) 0, (B) 0.025, (C) 0.25, (D) 2.5, (E) 25, and (F) 100 μg mL^{-1} for 24 h. R1, R2, and R3 represent the regions of dead cells, late apoptotic cells, and early apoptotic cells, respectively.

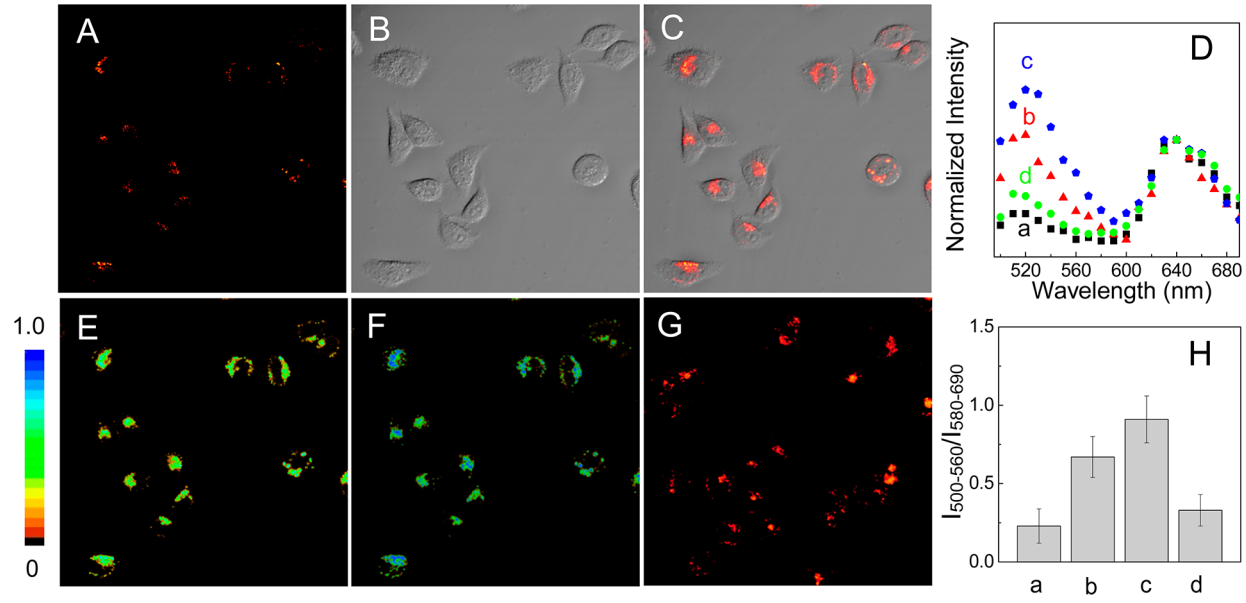

Figure 6. (A) Pseudocolored ratiometric images ($I_{500-560}/I_{580-690}$) of Hela cells with AuNC@HPF probes. (B) The bright-field image and (C) the overlay of confocal fluorescence image and the bright-field image of Hela cells before being exposed to $^{\bullet}$OH (generated by 10 μg mL^{-1} LPS) excited by 488 nm. (D) Normalized fluorescence emission scan from the AuNC@HPF probe in Hela cells (a) before addition of LPS, (b) after being stimulated by LPS for 45 min and (c) 90 min, and (d) in the presence of 0.1% DMSO before being stimulated by LPS for 90 min. (E–G) Pseudocolored ratiometric images ($I_{500-560}/I_{580-690}$) of Hela cells. (E and F) The ratio images of Hela cells with AuNC@HPF probes after being stimulated by LPS for 45 and 90 min, respectively. (G) The ratio image in the presence of 0.1% DMSO before being stimulated by LPS for 90 min. (H) A bar graph showing the integrated fluorescence intensity from 500 to 560 nm over the integrated intensity from 580 to 690 nm. Values are the mean ratios generated from the intensities from five randomly selected fields. The error bars represent standard error measurements (SEM) (a) before addition of LPS, (b) after being stimulated by LPS for 45 min and (c) 90 min, and (d) in the presence of 0.1% DMSO before being stimulated by LPS for 90 min.

We next sought to assess whether AuNC@HPF as a ratiometric probe could report changes in the $^{\bullet}$OH level in live cells by confocal fluorescence imaging. Upon excitation at 488 nm, the ratio images of Hela cells treated with AuNC@

dx.doi.org/10.1021/ac403810g | Anal. Chem. 2014, 86, 1829–1836

HPF were constructed from two collection channels (Figure S8 in the Supporting Information, 500−560 nm, I_{green} and 580−690 nm, I_{red}). From Figure 6C, we can see that the average emission ratio I_{green}/I_{red} is 0.23 ± 0.11, revealing very low level [the same concentration of •OH as generated by 1 ± 3 μM Fe^{2+} and the corresponding concentration of H_2O_2 (Fe^{2+}/H_2O_2 = 1:6)] of available •OH in the normal condition. Then, the I_{green}/I_{red} ratio increased to 0.67 ± 0.14 and 0.91 ± 0.15 when the cells incubated with AuNC@HPF probe were treated with LPS (a stimulator for production of ROS) for 45 and 90 min, respectively (Figure 6H), implying the generation of •OH in Hela cells (18 ± 3 and 29 ± 4 μM, Fe^{2+}/H_2O_2 = 1:6). The false color clearly changed from red to green, as demonstrated in Figure 6, parts A, E, and F. From the fluorescence images of separated channels as shown in Figure S8 in the Supporting Information, we can see that only the fluorescence of HPF changed with the reaction of •OH, while no obvious changes were observed for the AuNCs channel. In order to make sure the fluorescence enhancement of the HPF channel was actually due to the generation of •OH in cells, treatment of cells with an •OH scavenger, DMSO,[29] was carried out before the stimulation of LPS. As shown in Figure 6G, the fluorescence ratio maintained to 0.34 ± 0.09 (4 ± 2 μM, Fe^{2+}/H_2O_2 = 1:6), and false color also showed in red, indicating that the fluorescence ratio changes observed after being stimulated by LPS were ascribed to the generation of •OH in cells. These initial experiments in Hela cells demonstrated that we could observe the changes in •OH level in live cells through the fluorescence ratios of the developed ratiometric fluorescent biosensor, suggesting the great potential of the AuNC@HPF dual-emission probe for further fundamental biology research.

CONCLUSIONS

In summary, a ratiometric fluorescence sensor for •OH has been developed for bioiamging and biosensing in live cells, by using AuNCs as the reference signal and HPF acting as both the response signal and specific recognition element. The present fluorescent sensor exhibits high selectivity over typical ROS and RNS, metal ions, and other biological species, as well as good sensitivity, low detection limit, and high accuracy. Meanwhile, the AuNC-based inorganic−organic probe shows long-term stability against light illumination and pH, good cell permeability, low cytotoxicity, and high biocompatibility. Accordingly, the hybridized fluorescent biosensor with high analytical performance, together with the unique properties of AuNCs, has been successfully applied for bioimaging of •OH, and for the first time for monitoring the changes of •OH level in live cells under oxidative stress. This work has not only established a reliable and accurate approach to determination of •OH in a living system but also provided a methodology to designing the ratiometric sensors for other ROS and related species, which may play critical roles in the biological and pathological events.

ASSOCIATED CONTENT

Supporting Information

Quantum yield calculations, the optimized mass concentration ratio, reaction time, the reaction of probe with H_2O_2 or Fe^{2+}, the selectivity test against amino acids and glucose, pH stability, and nuclear staining experiments. This material is available free of charge via the Internet at http://pubs.acs.org.

AUTHOR INFORMATION

Corresponding Author

*E-mail: yangtian@tongji.edu.cn. Phone: +86-21-65987075. Fax: +86-21-65981097.

Notes

The authors declare no competing financial interest.

ACKNOWLEDGMENTS

This work was financially supported by the NSFC (21175098) and National Natural Science Fund for distinguished young scholars (21325521).

REFERENCES

(1) (a) Finkel, T.; Holbrook, N. J. *Nature* **2000**, *408*, 239−247. (b) Lisanti, M. P.; Martinez-Outschoorn, U. E.; Pavlides, S.; Whitaker-Menezes, D.; Pestell, R. G.; Howell, A.; Sotgia, F. *Cell Cycle* **2011**, *10*, 2059−2063. (c) Martindale, J. L.; Holbrook, N. J. *J. Cell. Physiol.* **2002**, *192*, 1−15. (d) Yang, K. D.; Shaio, M. F. *Biochem. Biophys. Res. Commun.* **1994**, *200*, 1650−1657. (e) Liu, H.; Tian, Y.; Xia, P. *Langmuir* **2008**, *24*, 6359−6366. (f) Deng, Z.; Rui, Q.; Yin, X.; Liu, H.; Tian, Y. *Anal. Chem.* **2008**, *80*, 5839−5846. (g) Luo, Y.; Liu, H.; Rui, Q.; Tian, Y. *Anal. Chem.* **2009**, *81*, 3035−3041. (h) Li, X.; Liu, Y.; Zhu, A.; Luo, Y.; Deng, Z.; Tian, Y. *Anal. Chem.* **2010**, *82*, 6512−6518.

(2) (a) Wiseman, H.; Halliwell, B. *Biochem. J.* **1996**, *313*, 17−29. (b) Cadet, J.; Berger, M.; Douki, T.; Ravanat, J.-L. *Rev. Physiol., Biochem. Pharmacol.* **1997**, *131*, 1−87.

(3) Toshiharu, A.-M.; Noboru, S.; Osafμmi, Y. *Br. J. Pharmacol.* **1999**, *126*, 1462−1470.

(4) Ren, J.-G.; Xia, H. L.; Just, T.; Dai, Y. R. *FEBS Lett.* **2001**, *488*, 123−132.

(5) (a) Oka, T.; Yamashita, S.; Midorikawa, M.; Saiki, S.; Muroya, Y.; Kamibayashi, M.; Yamashita, M.; Anzai, K.; Katsumura, Y. *Anal. Chem.* **2011**, *83*, 9600−9604. (b) Yim, M. B.; Chock, P. B.; Stadtman, E. R. *Proc. Natl. Acad. Sci. U.S.A.* **1990**, *87*, 5006−5010.

(6) Xue, Y.; Luan, Q.; Yang, D.; Yao, X.; Zhou, K. *J. Phys. Chem. C* **2011**, *115*, 4433−4438.

(7) (a) Zhu, A.; Liu, Y.; Rui, Q.; Tian, Y. *Chem. Commun.* **2011**, *47*, 4279−4281. (b) Li, L.; Zhu, A.; Tian, Y. *Chem. Commun.* **2013**, *49*, 1279−1281.

(8) Li, L.; Abe, Y.; Nagasawa, Y.; Kudo, R.; Usui, N.; Imai, K.; Mashino, T.; Mochizuki, M.; Miyata, N. *Biomed. Chromatogr.* **2004**, *18*, 470−474.

(9) Zhu, B.-Z.; Li, M.; Huang, C.-H.; Qin, H.; Fan, R.-M.; Kalyanaraman, B.; Zhu, J.-G. *Proc. Natl. Acad. Sci. U.S.A.* **2012**, *109*, 16046−16051.

(10) Huang, W. T.; Xie, W. Y.; Luo, H. Q.; Li, N. B. *J. Mater. Chem.* **2012**, *22*, 1477−1481.

(11) (a) Ding, C.; Zhu, A.; Tian, Y. *Acc. Chem. Res.* [Online early access]. DOI: 10.1021/ar400023s. Published Online: Aug 2, **2013**. http://pubs.acs.org. (b) Kong, B.; Zhu, A.; Ding, C.; Zhao, X.; Li, B.; Tian, Y. *Adv. Mater.* **2012**, *24*, 5844−5848. (c) Zhu, A.; Qu, Q.; Shao, X.; Kong, B.; Tian, Y. *Angew. Chem., Int. Ed.* **2012**, *51*, 7185−7189. (d) Leung, C.; Hong, Y.; Chen, S.; Zhao, E.; Lam, J.; Tang, B. Z. *J. Am. Chem. Soc.* **2013**, *135*, 62−65. (e) Wang, J.; Mei, J.; Hu, R.; Sun, J.; Qin, A.; Tang, B. Z. *J. Am. Chem. Soc.* **2012**, *134*, 9956−9966. (f) Tang, B.; Yu, F.; Li, P.; Tong, L.; Duan, X.; Xie, T.; Wang, X. *J. Am. Chem. Soc.* **2009**, *131*, 3016−3023.

(12) (a) Yapici, N. B.; Jockusch, S.; Moscatelli, A.; Mandalapu, S. R.; Itagaki, Y.; Bates, D. K.; Wiseman, S.; Gibson, K. M.; Turro, N. J.; Bi, L. *Org. Lett.* **2012**, *14*, 50−53. (b) Li, P.; Xie, T.; Duan, X.; Yu, F.; Wang, X.; Tang, B. *Chem.—Eur. J.* **2010**, *16*, 1834−1840. (c) Tang, B.; Zhang, N.; Chen, Z.; Xu, K.; Zhuo, L.; An, L.; Yang, G. *Chem.—Eur. J.* **2008**, *14*, 522−528.

(13) (a) Setsukinai, K.; Urano, Y.; Kakinuma, K.; Majima, H. J.; Nagano, T. *J. Biol. Chem.* **2003**, *278*, 3170−3175. (b) Tachikawa, T.; Majima, T. *Langmuir* **2009**, *25*, 7791−7802. (c) Naito, K.; Tachikawa, T.; Fujitsuka, M.; Majima, T. *J. Phys. Chem. C* **2008**, *112*, 1048−1059.

(14) (a) Gross, E.; Liu, J. H.; Alayoglu, S.; Marcus, M. A.; Fakra, S. C.; Toste, F. D.; Somorjai, G. A. *J. Am. Chem. Soc.* **2013**, *135*, 3881−3886. (b) Liu, Y.; Ai, K.; Cheng, X.; Huo, L.; Lu, L. *Adv. Funct. Mater.* **2010**, *20*, 951−956. (c) Wang, Y.; Chen, J.-T.; Yan, X.-P. *Anal. Chem.* **2013**, *85*, 2529−2535. (d) Wang, Y.; Chen, J.; Irudayaraj, J. *ACS Nano* **2011**, *5*, 9718−9725.
(15) Lin, C.-A. J.; Yang, T.-Y.; Lee, C.-H.; Huang, S. H.; Sperling, R. A.; Zanella, M.; Li, J. K.; Shen, J.-L.; Wang, H.-H.; Yeh, H.-I.; Parak, W. J.; Chang, W. H. *ACS Nano* **2009**, *3*, 395−401.
(16) (a) Xie, J.; Zheng, Y.; Ying, J. Y. *J. Am. Chem. Soc.* **2009**, *131*, 888−889. (b) Wen, F.; Dong, Y.; Feng, L.; Wang, S.; Zhang, S.; Zhang, X. *Anal. Chem.* **2011**, *83*, 1193−1196.
(17) (a) Guével, X. L.; Trouillet, V.; Spies, C.; Li, K.; Laaksonen, T.; Auerbach, D.; Jung, G.; Schneider, M. *Nanoscale* **2012**, *4*, 7624−7631. (b) Chen, C.-T.; Chen, W.-J.; Liu, C.-Z.; Chang, L.-Y.; Chen, Y.-C. *Chem. Commun.* **2009**, 7515−7517.
(18) (a) Lee, D.; Donkers, R. L.; Wang, G.; Harper, A. S.; Murray, R. W. *J. Am. Chem. Soc.* **2004**, *126*, 6193−6199. (b) Negishi, Y.; Tsukuda, T. *Chem. Phys. Lett.* **2004**, *383*, 161−165.
(19) Wang, H.-H.; Lin, C.-A. J.; Lee, C.-H.; Lin, Y.-C.; Tseng, Y.-M.; Hsieh, C.-L. *ACS Nano* **2011**, *5*, 4337−4344.
(20) Ganea, G. M.; Kolic, P. E.; El-Zahab, B.; Warner, I. M. *Anal. Chem.* **2011**, *83*, 2576−2581.
(21) Soh, N.; Makihara, K.; Sakoda, E.; Imato, T. *Chem. Commun.* **2004**, 496−497.
(22) Yuan, L.; Lin, W.; Song, J. *Chem. Commun.* **2010**, *46*, 7930−7932.
(23) King, M.; Kopelman, R. *Sens. Actuators, B* **2003**, *90*, 76−81.
(24) Zhang, Z.; Luo, Q.; Yan, X.; Li, Z.; Luo, Y.; Yang, L.; Zhang, B.; Chen, H.; Wang, Q. *Anal. Chem.* **2012**, *84*, 8946−8951. (b) Crivat, G.; Kikuchi, K.; Nagano, T.; Priel, T.; Hershfinkel, M.; Sekler, I.; Rosenzweig, N.; Rosenzweig, Z. *Anal. Chem.* **2006**, *78*, 5799−5804.
(25) Lee, H.; Lee, K.; Kim, I.; Park, T. *Adv. Funct. Mater.* **2009**, *19*, 1884−1890.
(26) (a) Zhou, J.; Booker, C.; Li, R.; Zhou, X.; Sham, T.-K.; Sun, X.; Ding, Z. *J. Am. Chem. Soc.* **2007**, *129*, 744−745. (b) Karstens, T.; Kobs, K. *J. Phys. Chem.* **1980**, *84*, 1871−1872.
(27) Heyne, B.; Maurel, V.; Scaiano, J. C. *Org. Biomol. Chem.* **2006**, *4*, 802−807.
(28) (a) Goodell, M. A.; Rosenzweig, M.; Kim, H.; Marks, D. F.; DeMaria, M.; Paradis, G.; Grupp, S. A.; Sieff, C. A.; Mulligan, R. C.; Johnson, R. P. *Nat. Med.* **1997**, *3*, 1337−1345. (b) Pitter, D. R. G.; Wigenius, J.; Brown, A. S.; Baker, J. D.; Westerlund, F.; Wilson, J. N. *Org. Lett.* **2013**, *15*, 1330−1333.
(29) (a) Klein, S. M.; Cohen, G.; Cederbaum, A. I. *Biochemistry* **1981**, *20*, 6006−6012. (b) Li, B.; Gutierrez, P. L.; Blough, N. V. *Anal. Chem.* **1997**, *69*, 4295−4300.